A Linear Least-Squares Algorithm for Double-Wiebe Functions Applied to Spark-Assisted Compression Ignition

Erik Hellström
University of Michigan,
Ann Arbor, MI 48109
e-mail: erikhe@umich.edu

Anna Stefanopoulou
University of Michigan,
Ann Arbor, MI 48109
e-mail: annastef@umich.edu

Li Jiang
Robert Bosch LLC,
Farmington Hills, MI 48331
e-mail: li.jiang@us.bosch.com

An algorithm for determining the four tuning parameters in a double-Wiebe description of the combustion process in spark-assisted compression ignition engines is presented where the novelty is that the tuning problem is posed as a weighted linear least-squares problem. The approach is applied and shown to describe well an extensive data set from a light-duty gasoline engine for various engine speeds and loads. Correlations are suggested for the four parameters based on the results, which illustrates how the double-Wiebe approach can also be utilized in a predictive simulation. The effectiveness of the methodology is quantified by the accuracy for describing and predicting the heat release rate and predicting the cylinder pressure. The root-mean square errors between the measured and predicted cylinder pressures are 1bar or less, which corresponds to 2% or less of the peak cylinder pressure. [DOI: 10.1115/1.4027277]

1 Introduction

Controlled autoignition, or homogeneous charge compression ignition (HCCI), enables a fuel-efficient combustion with low nitric oxides and particulates due to the fast heat release and the homogeneous and dilute mixture [1,2]. The operating range of the engine is, however, limited and transient control is more challenging compared to more traditional combustion concepts [3]. The focus here is on spark-assisted compression ignition (SACI) combustion, where the HCCI is augmented with spark ignition, which has been shown to increase the load range and increase the control authority over the combustion phasing [4–7]. Spark-assisted compression ignition can also serve as a way of transitioning between HCCI and spark ignition (SI) combustion [8,9].

Analytic approximations of the combustion process, such as the Wiebe function, are computationally efficient and useful for analysis and control-oriented model development. The Wiebe function is one of the best-known approximations for the burn rate and has been applied to many varieties of internal combustion engines [10] and SACI, in particular [11]. Due to the simplicity of the approximation, the function parameters must be tuned to the experimental data and typically depend on several operating condition variables. The aim here is to utilize a double-Wiebe description of the SACI combustion and develop a fast and robust tuning algorithm. To this end, a double-Wiebe function is formulated with four parameters determined by a weighted linear least-squares problem. The parameterization is evaluated on experimental heat release data based on in-cylinder pressure measurements.

Double-Wiebe models first appeared for direct-injected diesel engines [10,12,13] for capturing the premixed and the diffusion combustion, respectively. Systematic tuning of the parameters was done in Ref. [14] using the nonlinear optimization method of line search in the steepest descent direction and where the data points were weighted to obtain a good fit around the maximum heat release rate. For HCCI combustion, a second Wiebe function was included in Ref. [15] for capturing the slower final phase of the combustion, which is attributed to cooler regions in boundary layers and crevices. A sweep of the parameter values was used for determining the best fit. A double-Wiebe function was applied to SACI combustion in Ref. [16] for estimating the fraction of the heat release from flame propagation and autoignition, respectively. The five parameters were determined using constrained nonlinear optimization and it was noted that the constraints must be carefully chosen and that the choice depends on the operating conditions. A model for SACI combustion is developed in Ref. [11] where two separate Wiebe functions, each with two parameters, are employed for the heat release. The parameters switch values at a point determined by an autoignition model. The calibrated values are tabulated as functions of the engine load, speed, and normalized air-fuel ratio. Nonlinear optimization techniques, in general, require an iterative search for the best parameters and do not guarantee that the globally optimal solution is found. The current work develops a double-Wiebe approximation for SACI combustion with four parameters together with an easily implementable unconstrained weighted linear least-squares tuning algorithm where the unique solution is explicitly calculated.

The paper is organized as follows. The algorithm is first motivated and described in detail. After that, the results using the experimental data are shown and discussed and conclusions are drawn.

2 Algorithm

The well-known Wiebe function was developed by Ivan Wiebe for diesel engine combustion in his 1932 dissertation; see the review in Ref. [10]. The function for the accumulated heat release is

$$x(\varphi; m, d) = 1 - \exp\left[a\left(\frac{\varphi}{d}\right)^{m+1}\right] \tag{1}$$

where the duration d and the characteristic exponent m are the parameters and a is chosen such that $x(d)$ has a desired value. Wiebe

Contributed by the Combustion and Fuels Committee of ASME for publication in the Journal of Engineering for Gas Turbines and Power. Manuscript received February 15, 2014; final manuscript received February 16, 2014; published online May 5, 2014. Editor: David Wisler.

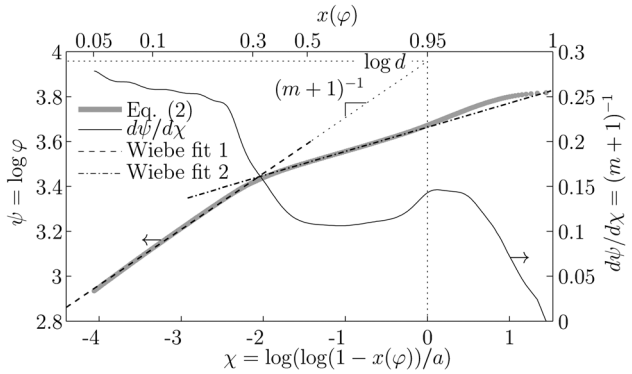

Fig. 1 SACI combustion heat release data transformed using Eq. (2) to show the linear regions

chose $x(d) = 99.9\%$ which yields $a \approx -6.908$. The parameters (d, m) are determined given a normalized heat release curve $x(\varphi)$ obtained by, e.g., pressure-based heat release analysis. Following the original work by Wiebe, Eq. (1) is rewritten, with algebra and using the logarithm twice, as

$$\log\varphi = \frac{1}{m+1}\log\left[\frac{1}{a}\log(1-x(\varphi))\right] + \log d \tag{2}$$

where the unknowns $(m+1)^{-1}$ and $\log d$ appear linearly in the known quantities. In the plot with $\psi = \log\varphi$ versus $\chi = \log[(1/a)\log(1-x(\varphi))]$, the parameters are thus determined by the slope and intercept of the linear approximation of the data. From Eq. (2), the parameters can be determined by a linear least-squares minimization problem, which is clearly advantageous compared to using Eq. (1) directly where the parameters enter in a nonlinear way and a nonlinear optimization algorithm is required. Here, a weighted least-squares is used, which for N data points is

$$\min_p \sum_{k=1}^{N} \gamma_k \left(\psi_k - \hat{\psi}(\chi_k; p)\right)^2 \tag{3}$$

where the index k denotes the data point, γ_k is the associated weight, $p = (\log d, (m+1)^{-1})^T$ is the parameter vector, and

$$\hat{\psi}(\chi_k; p) = Ap \tag{4}$$

where the rows of the matrix A are $A_k = (\chi_k, 1)$. The solution[1] is

$$\hat{p} = \left(A^T\Gamma A\right)^{-1} A^T\Gamma\Psi \tag{5}$$

with the matrices $\Gamma = \mathrm{diag}(\gamma_k)$ and $\Psi = (\psi_k)$ for $k = 1\ldots N$.

The transformation (2) is also useful for a multiple-Wiebe approach since it shows how one Wiebe function describes the data locally. Figure 1 shows an example with data from SACI combustion. The figure shows a common characteristic seen for the SACI where the data points follow a linear trend but the slope and intercept change fairly quickly during combustion; this occurs around $\chi = -2$ or $x = 30\%$ on the horizontal axis in Fig. 1. At this point, the slope $d\psi/d\chi$, which is also shown in the figure, and the intercept reduce, which means that the duration d decreases and the characteristic exponent m increases. The behavior corresponds to the understanding of the SACI as nearly a two-stage combustion, where a propagation flame combustion transitions to, and is quickly dominated by, a relatively faster autoignition [6,17]. As is obvious in the figure, a double-Wiebe description can fit the data much better than a single Wiebe.

[1]The solution is obtained by differentiating the criterion in Eq. (3) with respect to p, setting the result to zero, and solve for p.

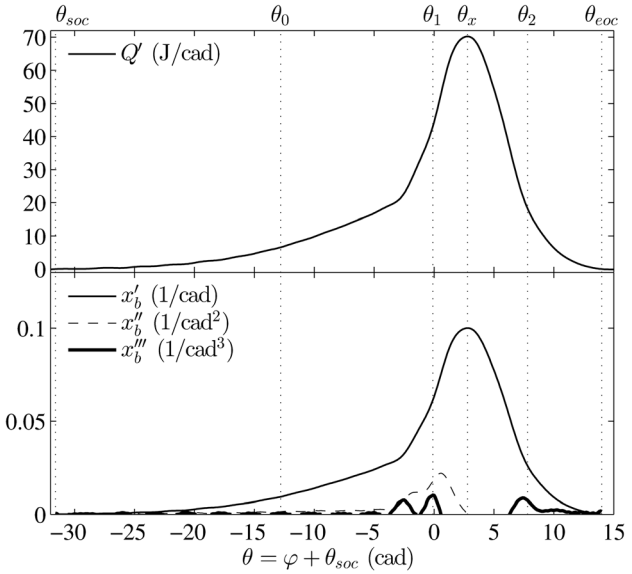

Fig. 2 The heat release rate Q' (top panel) and the first three derivatives of the burn fraction x_b (bottom panel). The transition angle θ_1 is defined at the peak value of x_b''' between θ_0 and θ_x, the peak of x_b'.

Towards the end of combustion, at around $x = 95\%$ in the upper right corner of Fig. 1, the trend changes again. Between, approximately, $x = 96\%$ and 99% the slope is at a higher level and, for the last percent of burn, the slope decreases towards zero. A slower burn at the end of autoignition, here between 96% and 99%, is consistent with observations in pure HCCI combustion and is attributed to cooler regions in the boundary layers and crevices [15]. Additional improvement for the SACI combustion could thus be obtained with a third Wiebe function, at the expense of a more complex description. The behavior in Fig. 1 for the last percent is a consequence of the fact that the estimated burn fraction goes to exactly one while the Wiebe function 1 only goes to one asymptotically as $\varphi \to \infty$. It can also be noted that the uncertainty in the heat release analysis is relatively larger late and early in the combustion than otherwise, since the ratio between the actual heat release and noise, from measurements and uncertainties in the parameters for, e.g., heat transfer models, is relatively lower. It is, therefore, generally wise to limit the interval used for data fitting or use weights in the error norm, which was done in, e.g., Ref. [14].

Based on the preceding observations, the aim with the current work is to utilize a double-Wiebe function for describing the main features of the SACI combustion while retaining the desirable property that the parameters can be determined from a linear-least squares problem. The formulation should lend itself to both the prescription and prediction of the burn rate. The basic idea is to, relying on the fact that the transition is fast, divide the data into two regions, one for flame propagation and the other for autoignition, where each region is described by a single-Wiebe function and then join these functions. Such an algorithm is described in the remainder of this section.

2.1 Algorithm Description. The inputs to the algorithm are the heat release curve $Q(\theta)$, computed from in-cylinder pressure measurements, the parameters (F_0, F_2), and the weighting factors γ_k.

2.1.1 Scaling and Data Selection. The first steps, illustrated in Fig. 2, are to normalize the data, select the data for fitting, and determine the transition angle where the interval is divided for the respective Wiebe function. The heat release curve is normalized between θ_{soc} and θ_{eoc}, which is the start and end of combustion,

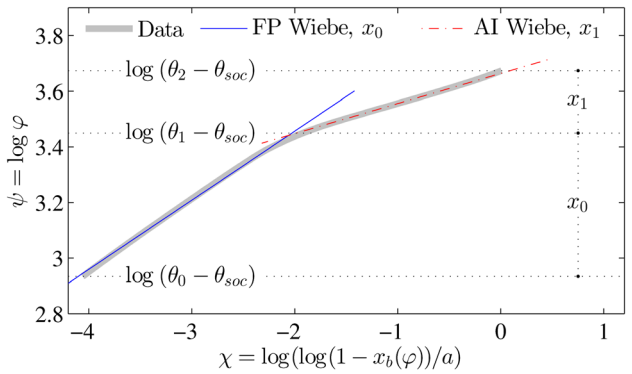

Fig. 3 Using Eq. (2) to determine the parameters for the flame propagation (FP) Wiebe function x_0 and the autoignition (AI) Wiebe function x_1, respectively

respectively, estimated from $Q(\theta)$. The local minimum before the main heat release and the maximum after are used to estimate θ_{soc} and θ_{eoc}, respectively. The normalized burn fraction curve is

$$x_b(\varphi), \quad \varphi = \theta - \theta_{soc} \tag{6}$$

where $x_b(0) = 0$ and $x_b(\theta_{eoc} - \theta_{soc}) = 1$. The data interval for fitting is restricted to

$$\theta \in (\theta_0, \theta_2) \text{ where } \theta_0 \in (\theta_{soc}, \theta_2) \tag{7}$$

where θ_0 and θ_2 are determined by where $Q(\theta)$ has reached $F_0\%$ and $F_2\%$ of its maximum value, respectively. The parameters (F_0, F_2) determine the data window used in the algorithm and limit the influence of the uncertainty in the very early and very late stages of combustion where the signal-to-noise ratio is low. The parameters here are chosen to be 5% and 95%, respectively. The transition angle θ_1 divides the interval into two regions, where each region is described by a Wiebe function and corresponds to when autoignition dominates the flame propagation. The transition point between flame propagation and autoignition was estimated in Ref. [18] by the maximum change of the slope of the heat release rate, i.e., the jerk (the third derivative) of the heat release. Here, it is also assumed that this occurs after θ_0 and before the angle of the peak heat release rate. The transition angle θ_1 is thus expressed by

$$\theta_1 = \arg\max_{\theta} \frac{d^3 x_b}{d\theta^3} \quad \text{s.t.} \quad \theta \in (\theta_0, \theta_x) \tag{8}$$

where

$$\theta_x = \arg\max_{\theta} \frac{dx_b}{d\theta} \tag{9}$$

2.1.2 Fit Wiebe Functions. The next step is to fit the two individual Wiebe functions $x_i(\varphi; d_i, m_i)$, $i = 0, 1$, with each having the form in Eq. (1), by computing the weighted linear-least squares solution in Eq. (5). The procedure is illustrated in Fig. 3. The parameters (d_0, m_0) in x_0, for the flame propagation, are fitted using the data in the interval (θ_0, θ_1) and (d_1, m_1) in x_1, for the autoignition, are fitted using the interval (θ_1, θ_2). The parameter a can arbitrarily be chosen for a desired interpretation of the parameter d. Here, it is chosen such that $x_i(d_i; m_i, d_i) = 95\%$, which yields $a \approx -2.996$. To improve the fit close to the peak heat release rate, the weights γ_k, $k = 1 \ldots N$ are chosen as

$$\gamma_k = \begin{cases} 100 & |\theta_k - \theta_x| < 2 \\ 0.01 & \text{otherwise} \end{cases} \tag{10}$$

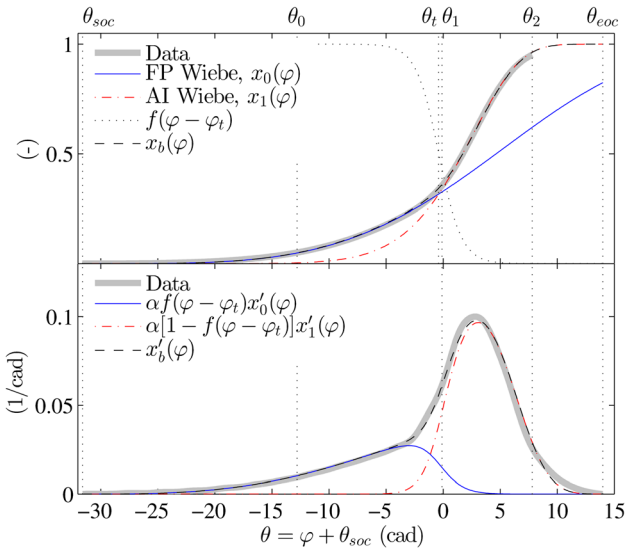

Fig. 4 Construction of the composite Wiebe function from Eqs. (11) and (14), by smoothly joining the two Wiebe functions

where θ_k denotes the crank angle for the data point k and θ_x, which isdefined in Eq. (9), denotes the location of the peak heat release rate.

2.1.3 Join Wiebe Functions. The final step is to join the Wiebe functions in order to obtain one composite function based on the individual functions x_0 and x_1. It should be noted that the reason the functions can be separately fitted and then joined is that the duration of the transition to autoignition is found to be short and independent of the operating conditions.

A smooth composite Wiebe function, which is completely described by the four parameters (d_0, m_0, d_1, m_1), is obtained by first joining the derivatives of the two functions through

$$x'(\varphi; d_0, m_0, d_1, m_1) = f(\varphi - \varphi_t)x_0'(\varphi; d_0, m_0) + [1 - f(\varphi - \varphi_t)]x_1'(\varphi; d_1, m_1) \tag{11}$$

where $f(\varphi)$ is an interpolation function between x_0 and x_1 describing the transition from flame propagation to autoignition combustion. The transition function is chosen as

$$f(\varphi) = \frac{1}{1 + e^{\varphi}} \tag{12}$$

Scaling the argument for the exponential controls how quickly the transition occurs and Eq. (12) was found to be appropriate for all data studied here. The angle φ_t corresponds to the transition angle and is chosen as the intersection between x_0 and x_1 given by

$$\varphi_t = \exp\left(\frac{\log\frac{d_0'}{d_1}}{r - 1}\right) \text{ where } r = \frac{m_0 + 1}{m_1 + 1} \tag{13}$$

Finally, the composite Wiebe function is given by

$$x_b(\varphi) = \alpha \int_0^{\varphi} x'(\tau) d\tau \tag{14}$$

where α is the normalization such that $x_b(\varphi) \to 1$, $\varphi \to \infty$. An illustration is given Fig. 4.

It should be noted that the fitting algorithm is independent of how the Wiebe functions are joined. The same algorithm can therefore be used for, e.g., model structures where there is an

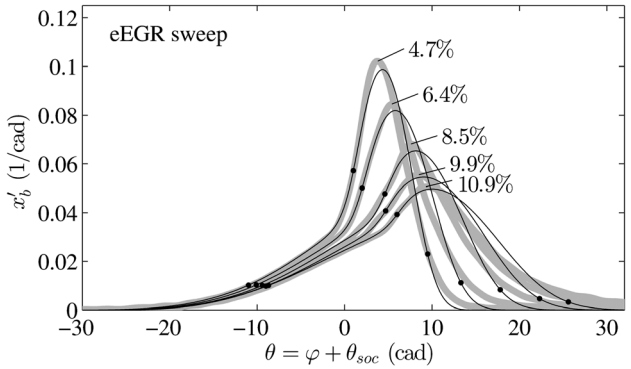

Fig. 5 Sweep of the eEGR at 5 bar BMEP and 2000 rpm. Data are shown with gray thick lines and fits with thin black lines. The dots mark the locations of θ_0, θ_1, and θ_2.

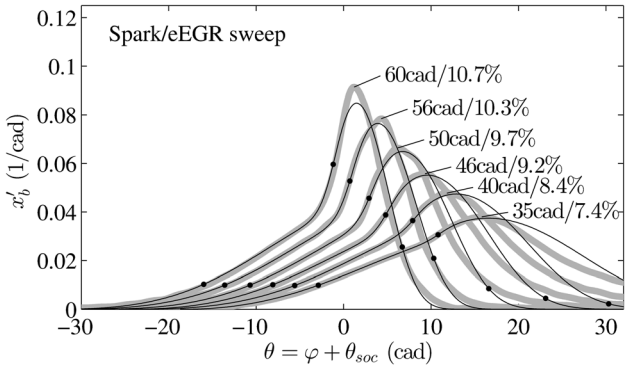

Fig. 6 Simultaneous sweep of the spark and eEGR at 5 bar BMEP and 2000 rpm. Data are shown with thick gray lines and fits with thin black lines. The dots mark the locations of θ_0, θ_1, and θ_2.

additional model predicting the transition point that depends on the flame propagation. One example is the piecewise function used in Ref. [11] that switches from x_0' to x_1' at a point given by an autoignition model instead of Eq. (13). Note, however, that simply switching between two functions will, in general, lead to a discontinuous heat release rate at $\varphi = \varphi_t$, while Eqs. (11)–(14) yield a smooth heat release with continuous derivatives.

2.2 Summary. The inputs to the algorithm are the heat release curve $Q(\theta)$ and the parameters (F_0, F_2, γ_k). The fitting procedure is summarized by the steps in Algorithm 1. The remaining step is to join the two Wiebe functions $x_0'(\varphi; d_0, m_0)$ and $x_1'(\varphi; d_1, m_1)$, which can be done in several ways. A smooth composite Wiebe function is obtained through Eqs. (11)–(14).

3 Experiments

The experiments were performed in a prototype four-cylinder 2.0 L engine, based on the GM Ecotec, running on Tier-II certification gasoline fuel. The compression ratio is 11, the bore and stroke is 86 mm, and the connecting rod is 146 mm. The prototype is designed for running multiple modes of combustion (such as HCCI, SACI, and SI) and the important features are a dual-lift valvetrain with dual-independent cam phasers, external exhaust gas recirculation (EGR), direct and port injection, and in-cylinder pressure sensors. The data presented here are from SACI combustion operated close to stoichiometry, with direct injection, and with the low cam lift profiles for intake and exhaust. Negative valve overlap is utilized to trap internal residual gas and a high-pressure EGR system provides cooled external residual gas.

A gross heat release analysis is performed on the average cylinder pressure, from 300 cycles, with a single-zone algorithm [19] following standard methods for analyzing cylinder pressure data.

Algorithm 1: Fit double-Wiebe function parameters:

(1) Choose the parameters F_0 and F_1, and the weights γ_k.
(2) Normalize the heat release curve $Q(\theta)$ between θ_{soc} and θ_{eoc}, which are the estimated start and end of combustion, respectively.
(3) Select the data interval for fitting as $\theta \in (\theta_0, \theta_2)$, where θ_i is chosen such that $Q(\theta_i) = F_i \max_\theta Q(\theta)$, $i = 0, 2$.
(4) Divide the interval at θ_1 where

$$\theta_1 = \arg\max_\theta \frac{d^3 x_b}{d\theta^3} \quad \text{s.t.} \quad \theta \in \left(\theta_0, \arg\max_\theta \frac{dx_b}{d\theta}\right)$$

and use the intervals (θ_0, θ_1) and (θ_1, θ_2) to fit the respective Wiebe function.
(5) Determine the parameters (d_i, m_i) in each of the functions

$$x_i(\varphi; d_i, m_i) = 1 - \exp\left[a\left(\frac{\varphi}{d_i}\right)^{m_i+1}\right], \quad i = 0, 1$$

where $\varphi = \theta - \theta_{soc}$ from the weighted linear least-squares solution

$$\left(\log d_i, (m_i + 1)^{-1}\right)^T = \left(A^T \Gamma A\right)^{-1} A^T \Gamma \Psi$$

with the matrices

$$A = (\chi_k, 1) = \left(\log\left[\frac{1}{a}\log(1 - x(\varphi_k))\right], 1\right)$$
$$\Gamma = \text{diag}(\gamma_k)$$
$$\Psi = (\psi_k) = (\log \varphi_k)$$

where $k = 1 \ldots N$ denotes the data point.

3.1 Results. To evaluate the quality of fit of the Wiebe functions the description in Eq. (11) is used, which only requires the four parameters fitted by the preceding algorithm. The results for cylinder 1 are shown here, the quality of the fits for the other cylinders is similar although the parameters are different due to variations between the cylinders.

A sweep of the external EGR (eEGR) is shown in Fig. 5. The eEGR valve was positioned at five different positions with other actuators held constant. When increasing the amount of the eEGR, which is cooled, the initial charge temperature drops and the autoignition event occurs later. The fit with the double-Wiebe function is fairly good overall and better for the lower eEGR. For more eEGR, the combustion is phased later and there is a larger fraction of the combustion occurring at a slower rate that is not captured by the second Wiebe function; see Fig. 1. The same observations are made in Fig. 6, which shows an experiment where the spark and eEGR were simultaneously changed. As the spark timing retards, the eEGR is decreased; the net effects are that the combustion duration increases, the autoignition occurs later, and the slower end phase of the combustion becomes longer.

The design of experiments (DOE) data with 107 points were used to see the quality of the fits for the SACI operating range. In the data set, the engine speed ranges from 1000 rpm to 3000 rpm and the load ranges from 2 bar to 6 bar brake mean effective pressure (BMEP). The eEGR valve, the start of injection, the intake and exhaust cam timings, and the spark timing are all simultaneously varied between different settings at each load and speed in the data set. Figure 7 shows a subset of the DOE data with a quality of fit that is representative for the entire DOE. The fits are fairly good over the range of loads and speeds. The quality of fit for each operating point is quantified by the average root-mean

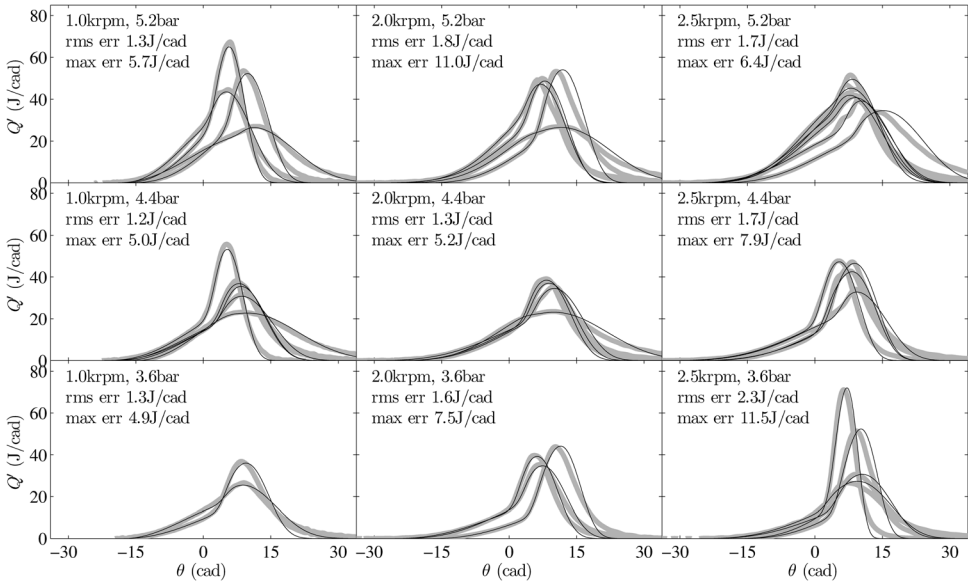

Fig. 7 Double-Wiebe function fits for a grid of engine speed, in krpm, and load, BMEP in bar. The different combustion characteristics at each operating point correspond to a multitude of conditions for various actuator settings (eEGR valve, start of injection, intake and exhaust cam timing, and spark timing) based on the chosen design of experiments. The root-mean-square (rms err) and maximum (max err) errors between the fitted curves (thin black lines) and measured data (thick gray lines) are computed for the interval $(\theta_{soc}, \theta_{eoc})$.

Table 1 Regressors (x_1, x_2) chosen for the DOE data set for the correlation in Eq. (16), which predicts the parameters (d_0, m_0, d_1, m_1) in the double-Wiebe function

Parameter	x_1	x_2
d_0	θ_s	iEGR
m_0	T_{ivc}	ϕ'
d_1	T_{ivc}	eEGR
m_1	T_{ivc}	eEGR

square (rms) error and the maximum error calculated between the start and end of combustion $(\theta_{soc}, \theta_{eoc})$. The rms error is below 2.3 J/cad and the maximum error is below 11.5 J/cad for all operating points.

3.1.1 Prediction. The resulting parameters from the algorithm have reasonable values and change in a well-behaved way between operating points. For all DOE data for cylinder 1, d_0 varies from 30 to 65, d_1 varies from 24 to 56, m_0 varies from 1.8 to 4.1, and m_1 varies from 1.8 to 8.8. Correlations for the parameters are developed by assuming that they, for a given speed and load, depend on the variables

$$\text{eEGR}, \text{iEGR}, T_{ivc}, x_b, \lambda, \theta_s, \phi' \tag{15}$$

where eEGR is the external EGR, iEGR is the internal EGR, T_{ivc} is the temperature at intake valve closing, x_b is the total burned gas fraction, λ is the normalized air-fuel ratio, θ_s is the spark timing, and $\phi' = (1 - x_b)/\lambda$ is the adjusted equivalence ratio defined in Ref. [20]. Linear correlations for the parameters

$$c_0 + c_1 x_1 + c_2 x_2 \tag{16}$$

were found to give a good fit where the regressors (x_1, x_2) are chosen among the terms (15) such that the total root-mean square error is minimized. The resulting regressors are shown in Table 1. It should be noted that this general technique may lead to other choices of regressors for another data set.

The value for m_0, which is the characteristic exponent for the flame propagation, could also be chosen constant, for each speed and load, without much deterioration of the fit.

The predicted heat release rates, with the double-Wiebe parameters computed from Eq. (16) using the regressors in Table 1, for the cases in Fig. 7 are shown in the top three rows of Fig. 8. As is expected, the errors compared to the data increase. The largest average rms error increases from 1 J/cad to 3.3 J/cad and the maximum error increases from 4.5 J/cad to 16.0 J/cad. To further quantify these errors, the cylinder pressure P is simulated using the predicted heat release. The simulation is based on the method used for the gross heat release analysis [19] described earlier, but instead of computing $Q(\theta)$ with $P(\theta)$ given, $P(\theta)$ is computed with $Q(\theta)$ specified by the predicted Wiebe function. The start of combustion, the total accumulated heat release, and the state at intake valve closing are used as input for the simulation. Therefore, the errors can solely be attributed to the predicted heat release rate. The simulated cylinder pressures, based on the double-Wiebe functions in the top three rows in Fig. 8, are shown in the bottom three rows in Fig. 8. The largest rms error is 1 bar and the largest maximum error is 3.4 bar, which is approximately 2% and 7% of the peak pressure, respectively.

3.2 Discussion. The algorithm produces double-Wiebe functions with an excellent fit for the flame propagation period and is fairly good for the autoignition period. For the autoignition period a perfect fit cannot be expected using all of the data (see the characteristics in Fig. 1), but the weights γ_k can be used to control where the emphasis is put. Another linear segment, a third Wiebe function, would improve the fit and could potentially be added in the current approach. A key question would be how to robustly determine the transition point to the final segment for curve fitting and how to predict the point in simulation. A suggestion for the former is to use the maximum jerk of the heat release after the peak heat release rate; compare with Eq. (8) and see Fig. 2. Moreover, due to the low signal-to-noise ratio late in the combustion, an accurate heat release analysis would be even more important.

From the correlation results based on the DOE it was seen that, for an operating point, the flame propagation part may be described by one varying parameter (d_0) while the autoignition

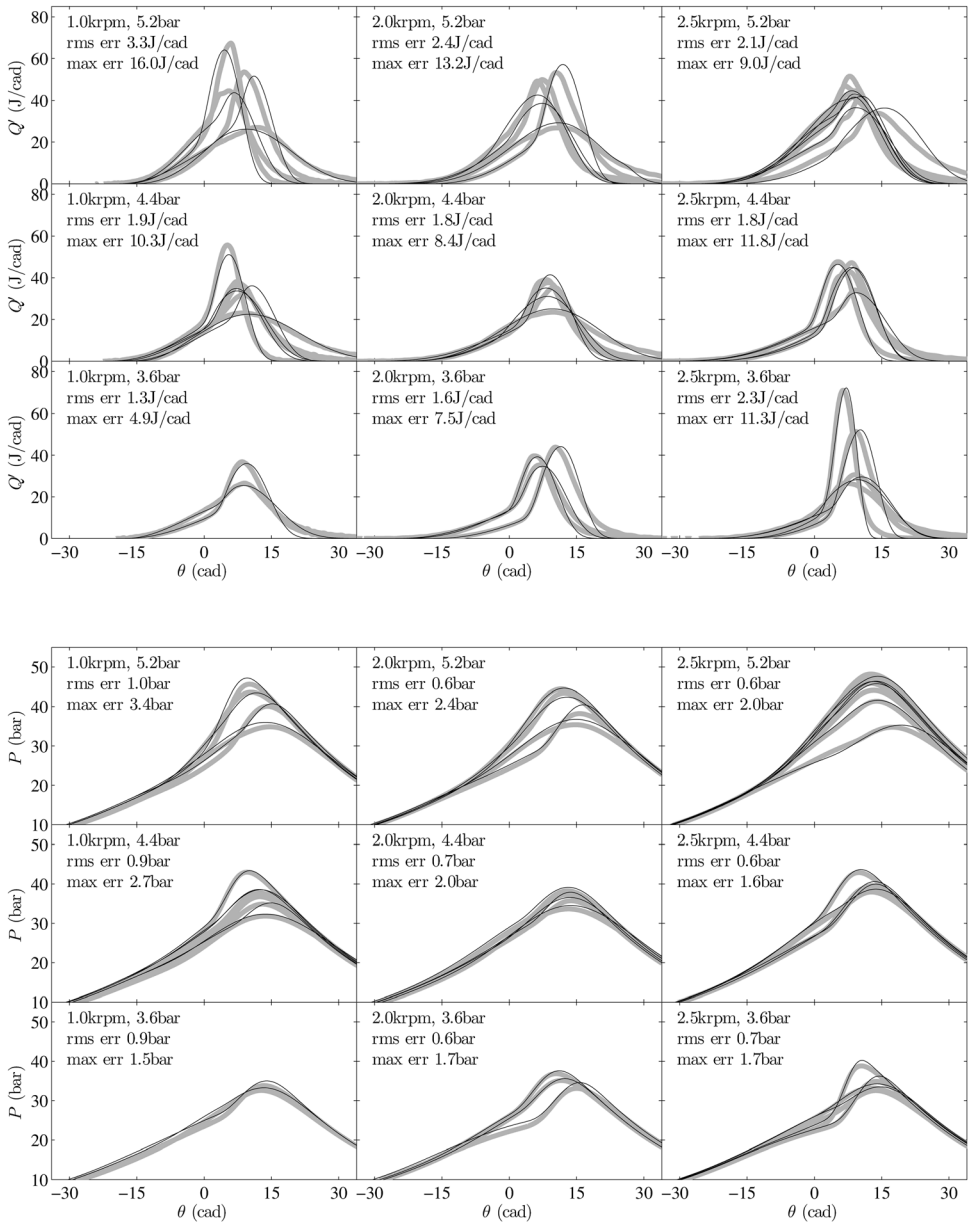

Fig. 8 Predicted heat release rate (top three rows) and predicted cylinder pressure (bottom three rows) are compared with data for varying engine speed, in krpm, and load, BMEP in bar. The root-mean-square (rms err) and maximum (max err) errors between the predicted curves (thin black lines) and measured data (thick gray lines) are computed for the interval $(\theta_{soc}, \theta_{eoc})$. The coefficients for the Wiebe functions are calculated from the regressors in Table 1 and the pressures are then simulated using the predicted heat release rate.

part requires two (m_1, d_1). This implies that the minimum data required for describing the shape are two coordinates, the angle φ_t and burn fraction x_t, at the transition point and one point on the autoignition part. For example, assuming that the 10% burn angle occurs in the flame propagation and the 90% angle in autoignition, the double-Wiebe function is uniquely characterized by the transition coordinate (φ_t, x_t) and the 10–90% burn duration. A combustion control strategy would thus need these two set points for complete control of the heat release rate. Since determining the transition point involves multiple differentiations of the pressure signal, using the 50% burn angle and the 10–90% duration is probably more practical for implementation.

4 Conclusions and Future Work

An algorithm is presented for fitting double-Wiebe functions that describe the SACI combustion process. The functions are formulated in a way such that the four parameters are uniquely determined from heat release data by a standard weighted linear least-squares problem. The algorithm is applied to the experimental data covering the operating range of SACI combustion in a light-duty gasoline engine. The results show that the double-Wiebe functions excellently match the data for the flame propagation and good for the autoignition part of the combustion. For the autoignition, there is a trade-off between accurately capturing the peak heat release rates and the slower final phase of the combustion. Correlations for the parameters are suggested, which enables the double-Wiebe parameterization to be integrated into predictive simulations. Cylinder pressure simulations, utilizing the correlations, show that the root-mean square error due to the double-Wiebe approximation of the heat release is 1 bar or less and the maximum error is 3.4 bar or less for the operating range. Future work may expand the correlations to explicitly include

load and speed variations and the approach may be extended with a third Wiebe function to better capture the final phase of the combustion.

Acknowledgment

David McKenna and Dan Polovina at AVL Inc., Farmington Hills, MI are thanked for providing the experimental data.

This work is supported by the Department of Energy (National Energy Technology Laboratory) under Award No. DE-EE0003533 and performed as a part of the ACCESS project consortium (Robert Bosch LLC, AVL Inc., Emitec Inc.) with direction from Hakan Yilmaz and Oliver Miersch-Wiemers, Robert Bosch, LLC.

References

[1] Najt, P. M. and Foster, D. E., 1983, "Compression-Ignited Homogeneous Charge Combustion," SAE Technical Paper 830264.
[2] Willand, J., Nieberding, R.-G., Vent, G., and Enderle, C., 1998, "The Knocking Syndrome—Its Cure and Its Potential," SAE Technical Paper 982483.
[3] Thring, R. H., 1989, "Homogeneous Charge Compression Ignition (HCCI) Engines," SAE Technical Paper 892068.
[4] Hyvönen, J., Haraldsson, G., and Johansson, B., 2005, "Operating Conditions Using Spark Assisted HCCI Combustion During Combustion Mode Transfer to SI in a Multi-Cylinder VCR-HCCI Engine," SAE Technical Paper 2005-01-0109.
[5] Kalian, N., Standing, R., and Zhao, H., 2005, "Effects of Ignition Timing on CAI Combustion in a Multi-Cylinder DI Gasoline Engine," SAE Technical Paper 2005-01-3720.
[6] Urushihara, T., Yamaguchi, K., Yoshizawa, K., and Itoh, T., 2005, "A Study of a Gasoline-Fueled Compression Ignition Engine—Expansion of HCCI Operation Range Using SI Combustion as a Trigger of Compression Ignition," SAE Technical Paper 2005-01-0180.
[7] Bunting, B. G., 2006, "Combustion, Control, and Fuel Effects in a Spark Assisted HCCI Engine Equipped With Variable Valve Timing," SAE Technical Paper 2006-01-0872.
[8] Wagner, R. M., Edwards, K. D., Daw, C. S., Green, J. B., Jr., and Bunting, B. G., 2006, "On the Nature of Cyclic Dispersion in Spark Assisted HCCI Combustion," SAE Technical Paper 2006-01-0418.
[9] Manofsky, L., Vavra, J., Assanis, D., and Babajimopoulos, A., 2011, "Bridging the Gap Between HCCI and SI: Spark-Assisted Compression Ignition," SAE Technical Paper 2011-01-1179.
[10] Ghojel, J. I., 2010, "Review of the Development and Applications of the Wiebe Function: A Tribute to the Contribution of Ivan Wiebe to Engine Research," Int. J. Engine Res., **11**(4), pp. 297–312.
[11] Yang, X. and Zhu, G. G., 2012, "A Control-Oriented Hybrid Combustion Model of a Homogeneous Charge Compression Ignition Capable Spark Ignition Engine," Proc. Inst. Mech. Eng., Part D: J. Automob. Eng., **226**(10), pp. 1380–1395.
[12] Ghojel, J. I., 1982, "A Study of Combustion Chamber Arrangements and Heat Release in D.I. Diesel Engines," SAE Technical Paper 821034.
[13] Miyamoto, N., Chikahisa, T., Murayama, T., and Sawyer, R., 1985, "Description and Analysis of Diesel Engine Rate of Combustion and Performance Using Wiebe's Functions," SAE Technical Paper 850107.
[14] Witt, H., Hassenforder, M., and Gissinger, G. L., 1995, "Modelling and Identification of a Diesel Combustion Process With the Downhill Gradient Search Method," SAE Technical Paper 950854.
[15] Yasar, H., Soyhan, H. S., Walmsley, H., Head, B., and Sorusbay, C., 2008, "Double-Wiebe Function: An Approach for Single-Zone HCCI Engine Modeling," Appl. Therm. Eng., **28**(11–12), pp. 1284–1290.
[16] Glewen, W. J., Wagner, R. M., Edwards, K. D., and Daw, C. S., 2009, "Analysis of Cyclic Variability in Spark-Assisted HCCI Combustion Using a Double Wiebe Function," Proc. Combust. Inst., **32**(2), pp. 2885–2892.
[17] Martz, J. B., Lavoie, G. A., Hong, H. I., Middleton, R. J., Babajimopoulos, A., and Assanis, D. N., 2012, "The Propagation of a Laminar Reaction Front During End-Gas Auto-Ignition," Combust. Flame, **159**(6), pp. 2077–2086.
[18] Persson, H., Hultqvist, A., Johansson, B., and Remon, A., 2007, "Investigation of the Early Flame Development in Spark Assisted HCCI Combustion Using High Speed Chemiluminescense Imaging," SAE Technical Paper 2007-01-0212.
[19] Hellström, E., Stefanopoulou, A. G., Vávra, J., Babajimopoulos, A., Assanis, D., Jiang, L., and Yilmaz, H., 2012, "Understanding the Dynamic Evolution of Cyclic Variability at the Operating Limits of HCCI Engines With Negative Valve Overlap," SAE Int. J. Engines, **5**(3), pp. 995–1008.
[20] Lavoie, G. A., Martz, J. B., Wooldridge, M., and Assanis, D., 2010, "A Multi-Mode Combustion Diagram for Spark Assisted Compression Ignition," Combust. Flame, **157**(6), pp. 1106–1110.